Implementation and analysis of a fuzzy logic and sliding mode controller on a Boost DC/DC converter

Benydir Mohamed *, Oubella M'hand*, Mouslim Sana*, Ajaamoum Mohamed *, Dahmane Kaoutar*, Imoudane Belkasem*

Laboratory of Engineering Sciences and Energy Management (LASIME), Ibn Zohr University, School National of Applied Sciences, 80000 Agadir Morocco

(mohamed.benydir@edu.uiz.ac.ma, m.oubella@uiz.ac.ma, sana.mouslim@uiz.ac.ma)

‡ Benydir Mohamed; Oubella M'hand, 80000 Agadir Morocco, Tel: +212 688 092 553, Fax: +212 661 162 246, mohamed.benydir@edu.uiz.ac.ma

Received: 27.01.2023 Accepted: 08.03.2023

Abstract- The DC/DC converters are primarily and practically used for switch-mode regulated power source and renewable energies such as photovoltaic or wind turbine. the principal purpose of these converters is to adapt the input with the output in other words, to preserve a consistent output voltage no matter the variations of the internal and external parameters of the converter. Different control techniques are commonly used to adapt and regulate the output voltage of these converters and make them more efficient and more robust in the event of unwanted disturbances, such as classic linear controllers for instance (proportional integrator and derivator controller PIDC) and nonlinear controllers as (fuzzy logic FLC, sliding mode controller SMC). This article presents a comparative performance of Fuzzy Logic Control (FLC) and Sliding Mode Control (SMC) on a DC/DC Boost converter submitted to different type of variations. The performance evaluation criteria depend on speed and precision of the transient response. The two proposed controllers are modeled, designed and simulated using MATLAB/SIMULINK. The results of the comparison between the two controllers confirm the effectiveness of sliding mode control in terms of rapidity and precision compared with FLC.

Keywords- Converters; sliding mode; fuzzy logic; nonlinear controller; robustness

1. Introduction

The grid connections always require suitable power converters to adapt the source to the load. A high-voltage DC grid must be connected to low-voltage renewable energy sources using a proper power electronic converter. A step-up converter is essential and adequate for the proposal, it is also more used for tracking the maximum power for photovoltaic power systems, it can ensure that the system operates with optimal efficiency despite the change of solar irradiation in the case of photovoltaic or the variation of wind speed in the case of wind turbine [1].

A proper control technique for DC/DC converters must take into consideration variations in internal parameters, large variations in input voltage and load, as well as ensure the stability under all operating conditions while providing fast response. There are several control techniques that have been suggested in the literature to achieve stability as well as fast transient response for all converter topologies, among these varied techniques, fuzzy logic control (FLC) and sliding mode (SMC) [19].

In [2] and [3] are focused on designing a PID controller for boost DC/DC converter, it provides a better voltage regulation and overshoot reduction with variation only on the input voltage. In [4,5,6] describes the design of fuzzy logic controller on DC/DC boost converter and buck boost converter compared to PID controller, FLC is more stable when varying with input voltage values. Also, in [1] a control technique called Model Predictive Control was used to regulate the output voltage of the converter, although it has a fast response with effective tracking but it is sensitive to circuit parameters. Recently, several papers [7,8,9] have proposed using SMC for DC/DC boost and buck converters compare to PI controller. The results tell that the SMC strategy offers important advantages such as fast dynamic response, strong robustness to load variations and simplicity in implementation [10]. However, most of the previous studies chose the variation of the input voltage or the variation of the load as disturbance in order to evaluate the robustness and stability, but do not take into considerations the variations of the internal parameters of the converters such as the inductive and capacitive components. So the values of C and L are carefully selected during the design phase of a converter to ensure that they meet the required specifications. However, changes in these values can occur over time, which may require adjustments to the converter design or operation to maintain optimal performance, since the main objective is to have a robust controller that works regardless of the type of variations. When sizing a DC/DC converter, the values of the parameters found are not always compatible with the standard values existing in the market, for that reason the controller chosen to regulate the output voltage must be stable despite the change in the value of the internal parameters [11].

In this paper, we will present firstly the sizing and mathematical modeling of a boost converter under continuous conduction mode. The converter operates in a scenario where the input voltage, inductor, capacitor and load values change causing a noticeable variation in the operating point of the DC/DC converter. The controller must ensure the stability of the converter despite of those unwanted disturbances. At first the converter submitted of variations in the input voltage with a range between 10 V and 18 V, then a variation of the load value at last, the internal values of the converter (capacitor and inductor) are subjected also to variations of ∓30\% of its dimensioning value. The results are used for designing and comparing the two controllers chosen, to regulate the output voltage [16].

The paper is structured as follow: the sizing and the mathematical modeling of the DC/DC boost converter in continuous conduction mode is given in second section. The proposed controllers are described and explained in the third section. The implementation and simulation results are presented in the fourth section. The finale section is dedicated to concluding remarks and discusses avenues for further research [15].

2. Sizing and Modeling of DC/DC Boost Converter

2.1. Sizing of Boost Converter

The boost converter is used frequently as non-isolated step-up converters which illustrated in Fig 1. This structure contains a continuous voltage source Vin, regulated switch T, inductor L, diode D, filter capacitor C and load resistance R. The operation of the converter will be studied under the continuous conduction mode CCM according to the state conduction of the switch T. R. The operation of the converter will be studied under the continuous conduction mode CCM according to the state conduction of the switch T.

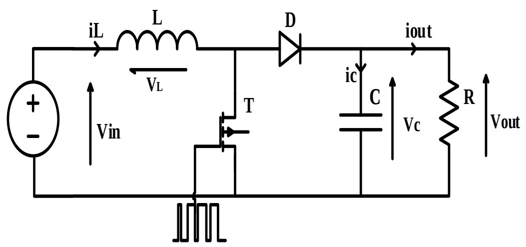

Fig. 1. Boost converter.

The main factor to be considered while designing any converter is the ripple current through the inductor, it typically varies from a 10\% up to 30\% [6]. The expression for ripple current is given as follows:

$$\Delta I_L = 10\% \times I_L \quad (1)$$

The duty cycle of the converter is expressed by the following formula:

$$\alpha = \frac{V_{out} - V_{in}}{V_{out}} \quad (2)$$

The value of the inductor L can be found by using the following expression:

$$L = \frac{\alpha \times V_{in}}{f \times \Delta I_L} \quad (3)$$

The value of capacitor C can be written as:

$$C = \frac{I_{out} \times \alpha}{f \times \Delta V_{out}} \quad (4)$$

the ripple of output voltage [12] is given by:

$$\Delta V_{out} = 1\% \times V_{out} \quad (5)$$

The sizing results of the different components of the boost converter are presented as follow:

- Input voltage V_{in}: 12V
- Output voltage V_{out}: 24V
- Switching frequency f : 10kHz
- Inductor L: 220µH
- Capacitor C: 600µF
- Resistive load R: 100Ω
- Duty cycle α: 0,5

2.2. Modeling of Boost Converter

Fig. 3 and Fig. 4 demonstrate the states conduction of the switch T of the boost converter. We will start the analysis by writing state space model of the boost converter during ON and OFF mode.

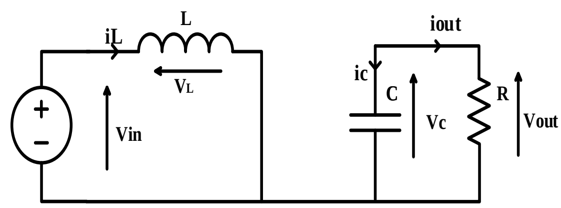

Fig. 2. Boost converter in ON mode.

As shown in Fig. 2, during the ON mode, the inductor is being charged by the input voltage source while the capacitor is discharging across the resistor. The equations are given as follows:

$$V_{in} - L\frac{di_L}{dt} = 0 \quad (6)$$

$$\frac{V_{out}}{R} - L\frac{dV_{out}}{dt} = 0 \quad (7)$$

The Eq. (6) and Eq. (7) can be written as follows:

$$\begin{bmatrix} \frac{di_L}{dt} \\ \frac{dV_{out}}{dt} \end{bmatrix} = \begin{bmatrix} 0 & 0 \\ 0 & \frac{-1}{RC} \end{bmatrix} \begin{bmatrix} i_L \\ V_{out} \end{bmatrix} + \begin{bmatrix} \frac{1}{L} \\ 0 \end{bmatrix} V_{in} \quad (8)$$

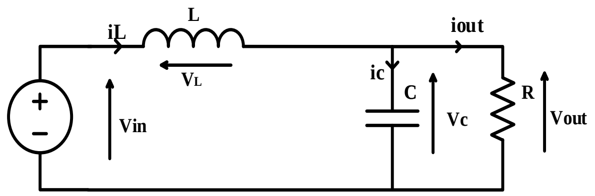

Fig. 3. Boost converter in OFF mode.

During OFF mode, the energy stored in the inductor is discharged by the diode to the output RC circuit. The equations can be given as follows:

$$V_{in} - V_{out} - L\frac{di_L}{dt} = 0 \qquad (9)$$

$$i_L - \frac{Vc}{R} - C\frac{dVout}{dt} = 0 \qquad (10)$$

Rearranging Eq. (9) and Eq. (10) to get the following state equation for the OFF mode:

$$\begin{bmatrix} \frac{di_L}{dt} \\ \frac{dV_{out}}{dt} \end{bmatrix} = \begin{bmatrix} 0 & \frac{-1}{L} \\ \frac{1}{C} & \frac{-1}{RC} \end{bmatrix} \begin{bmatrix} i_L \\ V_{out} \end{bmatrix} + \begin{bmatrix} \frac{1}{L} \\ 0 \end{bmatrix} V_{in} \qquad (11)$$

State space averaging technique serve to obtain a converter model over one switching period. In other words, it is required to replace the state space, which represents approximately the behaviour of the circuit over the entire period T [6]. Using state space averaging technique, the averaged modified model is given by:

$$A = A_1\alpha + A_2(1-\alpha) \qquad (12)$$

$$B = B_1\alpha + B_2(1-\alpha) \qquad (13)$$

Where A_1, A_1, B_1 and B_1 are given by:

$$A_1 = \begin{bmatrix} 0 & 0 \\ 0 & \frac{-1}{RC} \end{bmatrix} \qquad A_2 = \begin{bmatrix} 0 & \frac{-1}{L} \\ \frac{1}{C} & \frac{-1}{RC} \end{bmatrix}$$

$$B_1 = \begin{bmatrix} \frac{1}{L} \\ 0 \end{bmatrix} \qquad B_2 = \begin{bmatrix} \frac{1}{L} \\ 0 \end{bmatrix}$$

Using the above Eq. (12) and Eq. (13) to get the average space state model of the converter over the whole period T.

$$\begin{bmatrix} \frac{di_L}{dt} \\ \frac{dV_{out}}{dt} \end{bmatrix} = \begin{bmatrix} 0 & \frac{-(1-\alpha)}{L} \\ \frac{(1-\alpha)}{C} & \frac{-1}{RC} \end{bmatrix} \begin{bmatrix} i_L \\ V_{out} \end{bmatrix} + \begin{bmatrix} \frac{1}{L} \\ 0 \end{bmatrix} V_{in} \qquad (14)$$

Defining the state vector as:

$$x = [il \quad Vo]^T \qquad (15)$$

The equation (15) can be expressed as follows:

$$\dot{x} = Ax + BV_{in} \qquad (16)$$

$$y = Cx \qquad (17)$$

Where y is the output vector and:

$$A = \begin{bmatrix} 0 & -\frac{(1-\alpha)}{L} \\ \frac{1-\alpha}{C} & -\frac{1}{RC} \end{bmatrix} \qquad B = \begin{bmatrix} \frac{1}{L} \\ 0 \end{bmatrix} \qquad C = [0 \quad 1]$$

3. Controller Design

To demonstrate the performance of the proposed DC/DC boost converter, we must analyze the behavior of our converter in an open loop under MATLAB/Simulink with the parameters indicated before. The input voltage was initially set to 12 V, the voltage reference to 24 V and the resistive load set to 100 Ω.

Fig. 4 illustrates the simulation result of output voltage of the converter without controller.

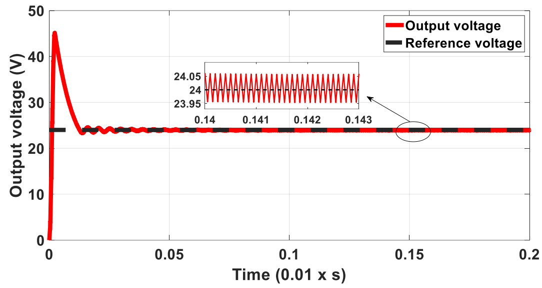

Fig. 4. The open loop response of the boost converter

After analysing the output voltage response of the converter, we can extract the performances of the transient response as peak overshoot ratio, rise time, peak time and settling time, the results are presented in below:

- Peak overshoot ration: 87.5%
- Rise time: 3,4 ms
- Peak time: 4,5 ms
- Settling time: 6,4 ms

Based on the simulation results obtained from Fig. 4, the open loop circuit respond has a high peak overshoot 87.5\% and an important settling time 6.4 ms that needs to reduce and improve. So, we can easily notice the necessity of a controller in order to improve the performances of the boost converter. The control parameters for DC/DC converters are the output voltage, input voltage, reference voltage and duty cycle.

3.1. Fuzzy Logic Controller

Fuzzy logic control (FLC) is a famous control technique which is based on artificial intelligence. The primary role of FLC is to implement decision rules by analyzing the system behavior and the input language variables, before generating any output from FLC, the inputs provided to the controller must go through three essential steps: fuzzification, inferences and defuzzification [13]. In the fuzzification phase, the input variables are transformed into linguistic variables using predefined membership functions (MFs). The output of the fuzzification step is then used to generate the fuzzified output according to the defined set of rules. Finally, in the defuzzification step, the fuzzy output is transformed into the required output used to control the converter [17].

FLC reads the output voltage value of the DC converter, the inputs are taken as the error e that is the difference between the actual value of the output voltage and the value of the setpoint voltage, and change in this error Δe, the output will be the duty cycle α of the Pulse Width Modeling PWM signal [14].

In Fig. 5, triangular membership functions (MFs) are employed for the FLC to make the computation easier.

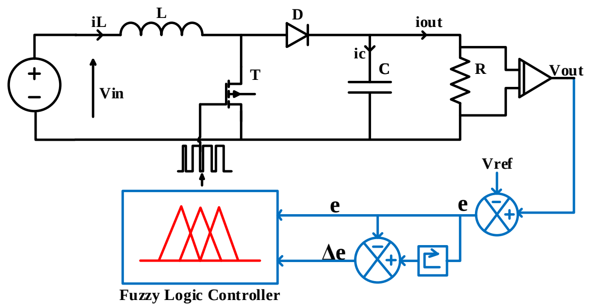

Fig. 5. Boost converter in close loop with FLC.

Table 1 shows the fuzzy rule table. The rules are in the form "If...Then", the "If" part is called the condition and the "Then" part is called the conclusion. the control strategy is structured in a natural language. Tree terms are used as linguistics variables: negative (N), zero (ZE) and positive (P) to describe each linguistic variable for both input variables e and Δe as well as output variable α [7].

Table 1. The rules of fuzzy logic

e / **Δ*e***	**N**	**Z**	**P**
N	P	P	P
Z	P	ZE	N
P	P	N	N

Figure 6 shows a group of the membership functions of the controller, these MFs take different shapes for example (Gaussian, triangular and trapezoids...), the most types used in the literature are triangles and trapezoids [14].

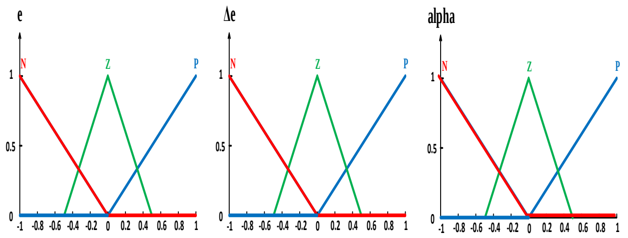

Fig. 6. Membership functions plots.

3.2. Sliding Mode Controller

Sliding Mode Control (SMC) is a non-linear type of control, which was originally introduced for the control of variable structural systems. Its main advantages are the guarantee of stability and robustness for wide variations in system parameters, input and disruptions on the system. The control strategy has two basic modes [18]. First one is the approach mode in which the trajectory moves to the slip line from any initial point and the second one is the sliding mode where the state trajectory moves to the origin along the switching line and the states do not leave it. In this study, we introduce the concept of the approaching mode [7]. The synthesis of a SMC can be summarized into several steps: The choice of the sliding surface, checking the attractiveness of the sliding surface, the demonstration of the existence of the sliding mode and the study of the stability of the control on the sliding surface [8].

The state variables are given as:

$$x=\begin{bmatrix}x_1\\x_2\\x_3\end{bmatrix}=\begin{bmatrix}V_{ref}-\beta V_{out}\\ \frac{d}{dt}(V_{ref}-\beta V_{out})\\ \int(V_{ref}-\beta V_{out})dt\end{bmatrix}\qquad(18)$$

x_1, x_2 and x_3 are respectively the voltage error, the derivative of the error and the integral of the error. V_{ref} and β are the reference voltage and the ratio of the voltage divider at the output of the converter. Considering Eq. (8), Eq. (11) and Eq. (15), the Eq. (20) can be re-expressed as follows:

$$x=\begin{bmatrix}x_1=V_{ref}-\beta V_{out}\\ x_2=\frac{\beta V_{out}}{RC}+\frac{\beta}{LC}\int(V_{ref}-V_{in})\bar{\alpha}dt\\ x_3=\int(V_{ref}-\beta V_{out})dt\end{bmatrix}\qquad(19)$$

The equation of state for the control system in the vector space are written in the following form:

$$\begin{bmatrix}\dot{x}_1\\\dot{x}_2\\\dot{x}_3\end{bmatrix}=\begin{bmatrix}0&1&0\\0&-\frac{1}{RC}&0\\1&0&0\end{bmatrix}\begin{bmatrix}x_1\\x_2\\x_3\end{bmatrix}+\begin{bmatrix}0\\\frac{\beta V_{out}}{RC}-\frac{\beta V_{in}}{LC}\\0\end{bmatrix}\bar{u}\qquad(20)$$

The SMC law indicates the switching function as follows:

$$u=\begin{cases}1, & \text{when }\gamma>0\\0, & \text{when }\gamma<0\end{cases}\qquad(21)$$

Where γ is the instantaneous state trajectory and is equal to:

$$\gamma=x_1\alpha_1+x_2\alpha_2+x_3\alpha_3=J^Tx\qquad(22)$$

$$J^T=[\alpha_1\ \alpha_2\ \alpha_3]$$

Where the Eq. (22) presents the sliding coefficients.

In order to drive the switch T of the converter by the pulse width modulation (PWM) technique, the two control signals V_c and a sawtooth signal V_r are compared, by setting the frequency of V_r identical to the signal frequency of PWM. In the first step, the equivalent control signal, u_{eq}, is obtained using the unsteady condition and in second step, during the process of deriving the trajectory of the instantaneous state γ, the equivalent control signal u_{eq} will be translated into PWM duty cycle.

$$\dot{\gamma}=J^TAx+J^TB\bar{u}_{eq}=0\qquad(23)$$

Were

$$\bar{u}_{eq}=-[J^TB]^{-1}J^TAx\qquad(24)$$

$$\bar{u}_{eq}=\frac{\beta L}{\beta(V_{out}-V_{in})}\left(\frac{\alpha_1}{\alpha_2}-\frac{1}{RC}\right)i_c-\frac{\alpha_3LC}{\alpha_2\beta(V_{out}-V_{in})}(V_{ref}-\beta V_{out})\qquad(25)$$

For this equation, $0<\bar{u}_{eq}<1$ by considering:

$$\bar{u}_{eq}=1-u_{eq}\qquad(26)$$

Eq. (26) can be summarized as follow:

$$0 < u_{eq} = \frac{-i_c \beta L\left(\frac{\alpha_1}{\alpha_2} - \frac{1}{RC}\right) + \frac{\alpha_3}{\alpha_2}(V_{ref} - \beta V_{out})LC + \beta(V_{out} - V_{in})}{\beta(V_{out} - V_{in})} < 1 \quad (27)$$

In a similar expression:

$$0 < u_{eq} = \frac{-K_{P1} i_c + K_{P1}(V_{ref} - \beta V_{out}) + \beta(V_{out} - V_{in})}{\beta(V_{out} - V_{in})} < 1 \quad (28)$$

$$0 < u_{eq} = \frac{V_c}{V_r} < 1 \quad (29)$$

Were

$$K_{P1} = \beta L\left(\frac{\alpha_1}{\alpha_2} - \frac{1}{RC}\right) \quad (30)$$

$$K_{P2} = \frac{\alpha_3}{\alpha_2} LC \quad (31)$$

By considering:

$$V_r = \beta(V_{out} - V_{in}) \quad (32)$$

The relation between V_c and V_r is defined. In relation to the damping coefficient and the settling time, the SMC coefficients can be determined [5].
Fig. 7 presents the boost converters and the controller circuits.

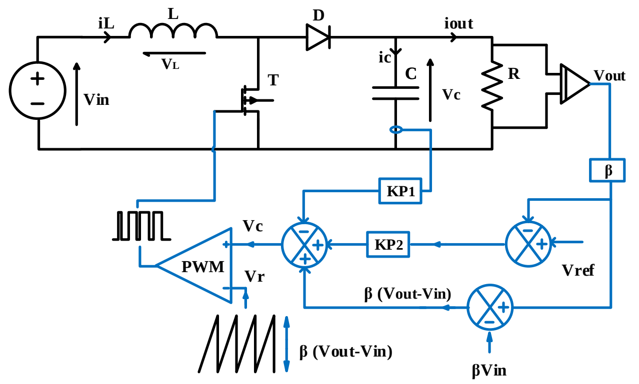

Fig. 7. Boost converter in close loop with SMC.

4. Simulation and Results

The results of the simulation for fuzzy logic controller and sliding mode controller on boost converter and the performances of both controllers have been validated using MATLAB/Simulink R2019a environment. The results are based on output voltage response, peak overshoot percentage, settling time and mean average precision (MAP) for both controllers.

Figure 8 is showing the output voltage response waveform of the boost converter under a constant input voltage, while being controlled by the FLC. The FLC is a type of controller that uses fuzzy logic to make decisions based on input variables. The waveform of the output voltage response that showen the changes in the output voltage over time as the input voltage remains constant at 12V

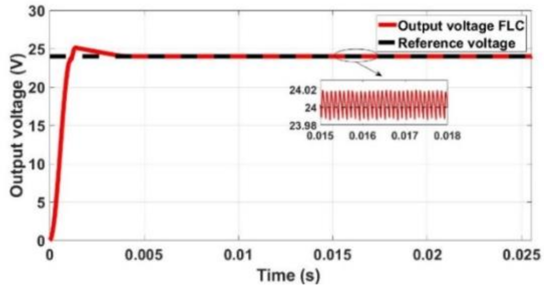

Figure 8. Output voltage response with FLC

İn Fig. 9 shows the output voltage response waveform of the boost converter with a variation in input voltage, while being controlled by the FLC. The input voltage is likely being varied within a specific range, and the waveform of the output voltage response shows the changes in the output voltage over time as the input voltage varies.

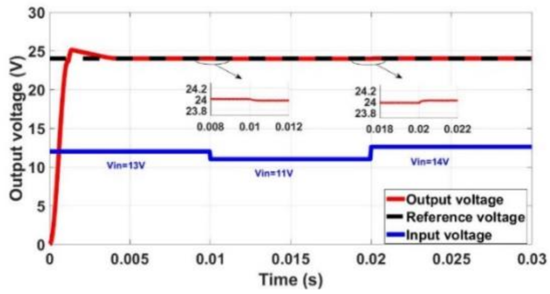

Fig. 9. Output voltage response with FLC under variation of Vin

In Fig.10 shows a graph that shows the response of a boost converter that is controlled by a sliding mode controller (SMC) when the input voltage is held constant.
Figure 11 reveals the response of the same boost converter as in Fig. 10, but with a different input voltage condition. Specifically, the input voltage is likely varied within a specific range to test the performance of the boost converter under varying voltage conditions.

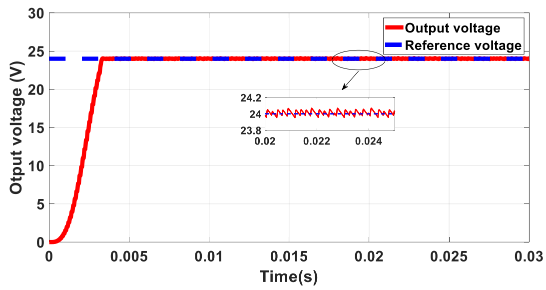

Fig. 10. Output voltage response with SMC

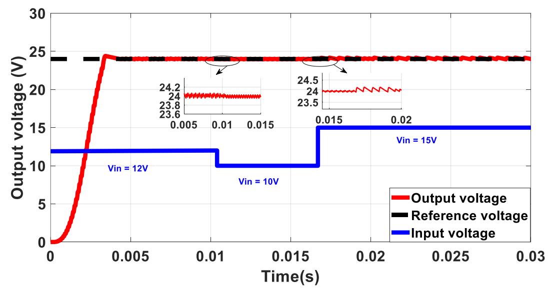

Fig. 11. Output voltage response with SMC under variation of Vin

The following Fig. 12 shows the response of the output voltage of the converter with the two controllers FLC and SMC. The purpose of the graph is to compare the performance of two different controllers, FLC and SMC, with respect to the output voltage of a converter. The response of the converter to each of these controllers is shown in the graph. The comparison is made in terms of two factors - rapidity and precision. Rapidity refers to how quickly the controllers can respond to changes in the input voltage and precision refers to how accurately they can maintain the desired output voltage.

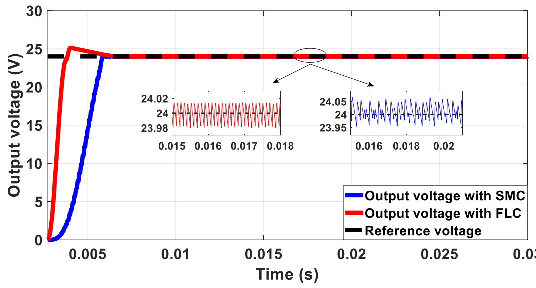

Fig. 12. Output voltage response with both controllers

In order to evaluate the precision of each controller, statistical analysis is performed using the mean absolute percentage error (MAPE) [6]. It can be calculated as the relative error, which is equal the absolute error between the output voltage value and the reference voltage divided by output voltage value as shown in the equation below:

$$\mathrm{MAPE} = \frac{1}{N}\sum_{t=t_0}^{N}\left|\frac{V_{out}-V_{in}}{V_{out}}\right| \times 100 \qquad (33)$$

The results of the mean absolute percentage error for the both controllers are presented in below:

- For FLC: MAPE = 8,8%
- For SMC: MAPE = 2,05%

Figures 13, 14 and 15 show the response of a boost converter that is controlled by an FLC (fuzzy logic controller) to variations in R (resistance), L (inductance), and C (capacitance). The boost converter is a type of DC-DC converter that steps up the voltage from its input to its output. The response of the converter refers to how it behaves in terms of its output voltage when changes are made to the input voltage or to the components in the converter circuit.

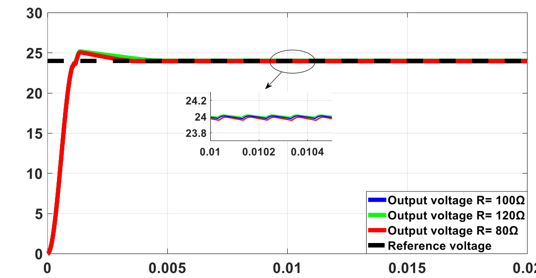

Fig. 13. Output voltage response with FLC under variations of R

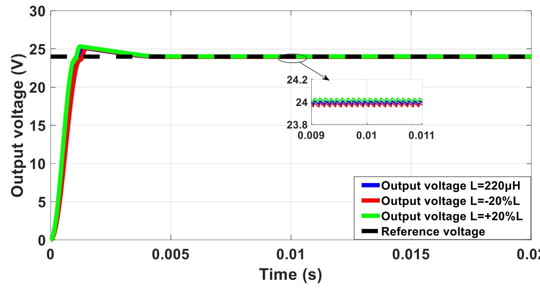

Fig. 14. Output voltage response with FLC under variations of L

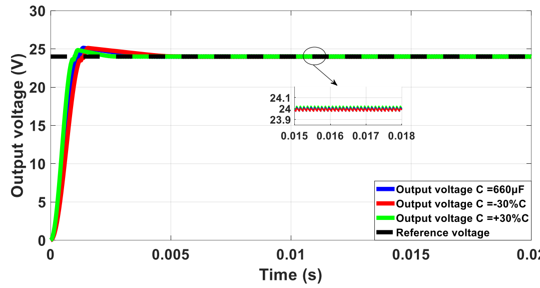

Fig. 15. Output voltage response with FLC under variations of C

Figures 16, 17 and 18 present the wave form of boost converter with SMC submitted to variations in R, L and C.

The output voltage response of a DC/DC Boost converter with sliding mode control (SMC) can be affected by changes in the value of the capacitor (C) or the inductance (L) used in the converter. Fig. 18 and Fig.17 show the waveform of the output voltage response of the converter with SMC under variations of C and L.

When the value of C is decreased, the output voltage response shows a faster rise time and settles to the desired output voltage value faster compared to the case when C is increased. This can be attributed to the fact that a smaller value of C leads to a higher charging current and a faster response of the converter. On the other hand, when the value of C is increased, the output voltage response shows a slower rise time and longer settling time to the desired output voltage value and same for the value of (L).

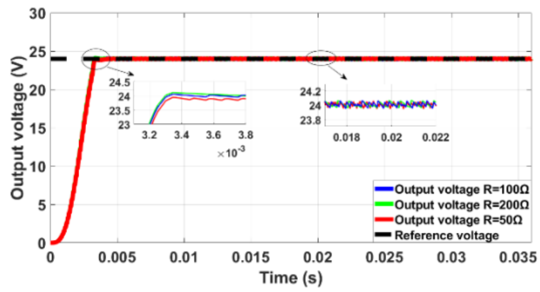

Fig.16. Output voltage response with SMC under variations of R

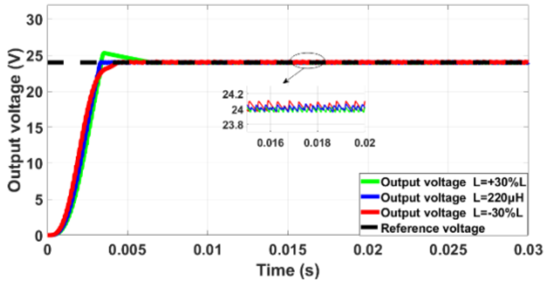

Fig. 17. Output voltage response with SMC under variations of L

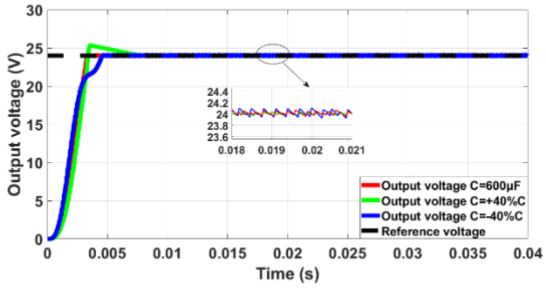

Fig. 18. Output voltage response with SMC under variations of C

According to the figures above, we can notice that the two control techniques give good performances, the overshoot is zero percent in the case of SMC and for FLC it is reduced to 4% and the response time has decreased from 6.4 ms to 5.6 ms for SMC and to 6.2 ms for FLC.

With a variation of the input voltage, the response perfectly follows the reference voltage with a small deviation of the output voltage on the moment of changing Vin, however SMC operates at a wide voltage range input voltage from 10 V to 18 V in comparison with FLC from 11 V to 15 V.

By varying the resistive load of the converter, it was observed that both FLC and SMC controllers are more stable. The SMC controller showed better tracking of the reference voltage and operates at a wider range of resistive values from 50 to 200, while FLC operates in the range of 80 to 120. Additionally, the internal values of the converter, such as the inductance L and the capacitor C, were also varied by ±20% and ±30%, respectively. It was found that despite the changes in the internal values, both controllers were able to track the desired output voltage value accurately, indicating their effectiveness in maintaining stability and precision. This is demonstrated in Fig. 16, Fig. 17 and Fig. 18 which show the waveforms of the boost converter with SMC under variations in R, L, and C.

Table 2 provides a summary of the performance comparison between two types of controllers (fuzzy logic controller and sliding mode controller) based on the characteristics of the transient response of a converter. The transient response of a converter refers to the behavior of the converter during the time it takes for the output to settle after a change in the input or load. The table includes information such as rise time, settling time, overshoot, and steady-state error of the output voltage for both types of controllers, which can be used to compare and evaluate their performance in regulating the output voltage of the converter.

Table 2. The comparison results of the two controllers

The controller	Without controller	FLC	SMC
Peak overshoot ration (%)	87.5	4,16	0
Rise time (ms)	3,4	3,7	5,6
Peak time (ms)	4,5	4	5,6
Settling time (ms)	6,4	6,2	5,6
Range of variation of Vin	-	12 V to 15 V	10 V to 18 V
MAPE (%)	15	8,8	2,05

5. Conclusion

This study aims to compare the performance of two different controllers, fuzzy logic controller (FLC) and sliding mode control (SMC), on a DC/DC boost converter. Both controllers were modeled, designed, and simulated using MATLAB/SIMULINK software. The results of the simulations showed that the sliding mode controller outperformed the fuzzy logic controller in terms of dynamic response. The SMC exhibited a fast transient response with almost zero overshoot ratio, which allowed it to achieve the desired output voltage of the boost converter quickly. Both controllers were found to be stable when varying with different input voltage. However, the SMC was able to operate under a wider range of input voltage, load, and internal converter components compared to the FLC. Thus, the SMC is more suitable for common DC/DC boost converter applications. The findings of this study can be used to inform the selection of an appropriate controller for a DC/DC boost converter system.

The two controllers proposed in this study have some limitations. The FLC requires rules to function properly despite not needing a mathematical model, resulting in a high computational load. On the other hand, the SMC suffers from a weakness known as the chattering phenomenon, which has been the focus of many research papers aiming to eliminate it using various methods. One such method involves designing a high-order slip mode control that can effectively eliminate chattering.

References

[1] F. Mumtaz, N. Zaihar Yahaya, S. Tanzim Meraj, B. Singh, R. Kannan, and O. Ibrahim, "Review on non-isolated DC-DC converters and their control techniques for renewable energy applications", Ain Shams Engineering Journal, vol. 12, no 4, p. 3747-3763, déc. 2021, doi: 10.1016/j.asej.2021.03.022.

[2] K. Sharma and D. K. Palwalia, "Design of digital PID controller for voltage mode control of DC-DC converters", in 2017 International conference on Microelectronic Devices, Circuits and Systems

(ICMDCS), Vellore, août 2017, p. 1-6. doi: 10.1109/ICMDCS.2017.8211715.

[3] M. R. Dave and K. C. Dave, “Analysis of Boost Converter Using PI Control Algorithms”, International Journal of Engineering Trends and Technology, p. 3, 2012.

[4] P. Hema Rani, S. Navasree, S. George, and S. Ashok, “Fuzzy logic supervisory controller for multi-input non-isolated DC to DC converter connected to DC grid”, International Journal of Electrical Power & Energy Systems, vol. 112, p. 49-60, nov. 2019, doi: 10.1016/j.ijepes.2019.04.018.

[5] N. F. N. Ismail, I. Musirin, R. Baharom, and D. Johari, “Fuzzy logic controller on DC/DC boost converter”, in 2010 IEEE International Conference on Power and Energy, Kuala Lumpur, Malaysia, nov. 2010, p. 661-666. doi: 10.1109/PECON.2010.5697663.

[6] S. Mouslim, “Simulation and analyses of SEPIC converter using linear PID and fuzzy logic controller” , Materials Today, p. 10.

[7] H. Guldemir, “Study of Sliding Mode Control of DC-DC Buck Converter”, EPE, vol. 03, no 04, p. 401-406, 2011, doi: 10.4236/epe.2011.34051.

[8] Q. Qi, D. Ghaderi, and J. M. Guerrero, “Sliding mode controller-based switched-capacitor-based high DC gain and low voltage stress DC-DC boost converter for photovoltaic applications”, International Journal of Electrical Power & Energy Systems, vol. 125, p. 106496, févr. 2021, doi: 10.1016/j.ijepes.2020.106496.

[9] C. S. Sachin and Sri. G. Nayak, “Design and simulation for sliding mode control in DC-DC boost converter”, in 2017 2nd International Conference on Communication and Electronics Systems (ICCES), Coimbatore, oct. 2017, p. 440-445. doi: 10.1109/CESYS.2017.8321317.

[10] H. Abidi and A. Mami, “Grid connected photovoltaic system controlled by SMC”, in 2016 4th International Conference on Control Engineering & Information Technology (CEIT), Hammamet, Tunisia, déc. 2016, p. 1-5. doi: 10.1109/CEIT.2016.7929106.

[11] K. Wang, D. Liu, and L. Wang, “The Implementation of Synergetic Control for a DC-DC Buck-Boost Converter”, Procedia Computer Science, vol. 199, p. 900-907, 2022, doi: 10.1016/j.procs.2022.01.113.

[12] M. Shadoul, R. A. Abri, H. Yousef, and M. Masoud, “DC- DC Boost Converter Controller Design for PV Applications”, in 2017 9th IEEE-GCC Conference and Exhibition (GCCCE), Manama, mai 2017, p. 1-6. doi: 10.1109/IEEEGCC.2017.8448164.

[13] H. A. Mosalam, R. A. Amer, and G. A. Morsy, “Fuzzy logic control for a grid-connected PV array through Z-source-inverter using maximum constant boost control method”, Ain Shams Engineering Journal, vol. 9, no 4, p. 2931-2941, déc. 2018, doi: 10.1016/j.asej.2018.10.001.

[14] P. Hema Rani, S. Navasree, S. George, and S. Ashok, “Fuzzy logic supervisory controller for multi-input non-isolated DC to DC converter connected to DC grid”, International Journal of Electrical Power & Energy Systems, vol. 112, p. 49-60, nov. 2019, doi: 10.1016/j.ijepes.2019.04.018.

[15] S. Vadi, F. B. Gurbuz, S. Sagiroglu and R. Bayindir, "Optimization of PI Based Buck-Boost Converter by Particle Swarm Optimization Algorithm," *2021 9th International Conference on Smart Grid (icSmartGrid)*, Setubal, Portugal, 2021, pp. 295-301, doi: 10.1109/icSmartGrid52357.2021.9551229.

[16] A. Belkaid, I. Colak, K. Kayisli, M. Sara and R. Bayindir, "Modeling and Simulation of Polycrystalline Silicon Photovoltaic Cells," *2019 7th International Conference on Smart Grid (icSmartGrid)*, Newcastle, NSW, Australia, 2019, pp. 155-158, doi: 10.1109/icSmartGrid48354.2019.8990733

[17] A. Belkaıd, I. Colak, K. Kayıslı and R. Bayındır, "Improving PV System Performance using High Efficiency Fuzzy Logic Control," *2020 8th International Conference on Smart Grid (icSmartGrid)*, Paris, France, 2020, pp. 152-156, doi: 10.1109/icSmartGrid49881.2020.9144817.

[18] M. Farida, S. Belkacem and I. Colak, "Fuzzy High Order Sliding Mode Control Based DPC of DFIG using SVM," *2021 9th International Conference on Smart Grid (icSmartGrid)*, Setubal, Portugal, 2021, pp.278-282,doi: 10.1109/icSmartGrid52357.2021.9551262.

[19] J. Wachter, L. Gröll and V. Hagenmeyer, "Adaptive Feedforward Control for DC/DC Converters in Microgrids - A Power Hardware in the Loop Study," *2021 9th International Conference on Smart Grid (icSmartGrid)*, Setubal, Portugal, 2021, pp. 49-56, doi: 10.1109/icSmartGrid52357.2021.9551250.